RSC Advances

PAPER

Cite this: *RSC Adv.*, 2023, **13**, 35349

Strategy to enhance the semicontinuous anaerobic digestion of food waste *via* exogenous additives: experimental and machine learning approaches†

Chuan Ding,[a] Yi Zhang,[a] Xindu Li,[a] Qiang Liu,[a] Yeqing Li, *[a] Yanjuan Lu,[b] Lu Feng,[c] Junting Pan[d] and Hongjun Zhou*[a]

Received 25th August 2023
Accepted 21st November 2023

DOI: 10.1039/d3ra05811e

rsc.li/rsc-advances

The anaerobic digestion (AD) of food waste (FW) was easy to acidify and accumulate ammonia nitrogen. Adding exogenous materials to the AD system can enhance its conversion efficiency by alleviating acidification and ammonia nitrogen inhibition. This work investigated the effects of the addition frequency and additive amount on the AD of FW with increasing organic loading rate (OLR). When the OLR was 3.0 g VS per L per day and the concentration of the additives was 0.5 g per L per day, the stable methane yield reached 263 ± 22 mL per g VS, which was higher than that of the group without the additives (189 mL per g VS). *Methanosaetaceae* was the dominant archaea, with a maximum abundance of 93.25%. Through machine learning analysis, it was found that the optimal daily methane yield could be achieved. When the OLR was within the range of 0–3.0 g VS per L per day, the pH was within the range of 7.6–8.0, and the additive concentration was more than 0.5 g per L per day. This study proposed a novel additive and determined its usage strategy for regulating the AD of FW through experimental and simulation approaches.

1. Introduction

In 2020, the total amount of municipal solid waste (MSW) will be 254.79 million tons in China, with a continuous growth rate of 5–6%.[1] Among them, food waste (FW) is the main source of MSW.[2] At present, the production of FW is steadily increasing.[3] In China, the output of FW accounted for 30–50% of MSW in 2020.[4] To date, common methods that are used to deal with FW in China include landfill and incineration; however, these methods face increasing economic and environmental pressure.[5] Therefore, it is necessary to study how to deal with FW in a harmless, reduced, and resourceful manner to achieve sustainable development. Anaerobic digestion (AD) is a technique that can effectively achieve the volume reduction and resourceful treatment of FW.[1] However, the continuous AD of FW will easily lead to the accumulation of volatile fatty acids (VFA) with an increase in organic loading rate (OLR). The accumulation of propionic/butyric acid is one of the crucial reasons for the acidification of the AD system. Because the oxidation of propionic acid/butyric acid is usually not spontaneous in thermodynamics, it requires hydrogenotrophic methanogens to continuously consume H_2 to maintain a low partial pressure ($<10^{-4}$–10^{-5} atm) to make propionic acid/butyric acid oxidation thermodynamically feasible. Therefore, how to promote the metabolism of methanogens is the key to solve the acidification.

In 2014, Lovley *et al.* discovered that *Geobacter* could directly oxidize ethanol and transfer the electrons through conductive mycelium[6] or c-type cytochromes[7] to *Metanothrix*[8] or *Metanosarcina*.[9] These methanogens receive electrons and then reduce CO_2 to CH_4. Compared to traditional methanogenesis, the direct interspecies electron transfer (DIET) pathway for methanogenesis has the following potential advantages: (1) complex organic matter can be directly metabolized into methane by DIET without hydrolysis and acidification. (2) Electron transfer does not require the diffusion of H_2, thus overcoming the thermodynamic limitations of converting organic compounds into acids. According to reports, exogenous materials can enhance AD by promoting electron transfer.[10] For instance, Cruz Viggi *et al.* found that conductive magnetite accelerated the conversion of propionic acid to methane in AD. In particular, previous studies have added conductive carbon cloth to high OLR AD systems (ethanol as substrate) to prevent acid accumulation.[11] The results showed that when the influent water was pH 5.0, the control group almost did not produce methane. In contrast, the methane production rate of the AD with carbon cloth was maintained at a high level

[a]*State Key Laboratory of Heavy Oil Processing, Beijing Key Laboratory of Biogas Upgrading Utilization, College of New Energy and Materials, China University of Petroleum Beijing (CUPB), Beijing 102249, P. R. China. E-mail: liyeqing@cup.edu.cn; zhhj63@163.com*

[b]*Beijing Fairyland Environmental Technology Co., Ltd, Beijing 100080, P. R. China*

[c]*Division of Environment and Natural Resources, Norwegian Institute of Bioeconomy Research (NIBIO), 1431 Ås, Norway*

[d]*State Key Laboratory of Efficient Utilization of Arid and Semi-arid Arable Land in Northern China, Institute of Agricultural Resources and Regional Planning, Chinese Academy of Agricultural Sciences, Beijing 100081, P. R. China*

† Electronic supplementary information (ESI) available. See DOI: https://doi.org/10.1039/d3ra05811e

(200 mL per day). When the pH is readjusted to 7.0, the performance of the AD with carbon cloth can be recovered to 85% of that before the pH adjustment, while the control group is only 23–33%. These results indicated that conductive materials can enhance the acid shock load of the AD system and accelerate the recovery to steady state by promoting DIET methanogenesis. In addition, FW has a high proportion of protein. High nitrogen-containing substances will release a large amount of ammonia nitrogen or free ammonia during AD, which can lead to damage to the microbial cell, pH imbalance, and enzyme inactivation. Some research studies have found that conductive materials, such as biochar[12] and magnetite,[13] can strengthen the AD to resist the impact of high-concentration ammonia nitrogen or free ammonia. Currently, most of these conductive materials were either derived from waste conversion or extracted to control costs. Consequently, it was often challenging to control the properties of the resulting products. Further modifications increased the complexity of the process and production costs.

Based on the above considerations, this study developed novel low-cost and orientation-control additives. A semi-continuous AD experiment was conducted to test the influence of the additives on the methane yield, VFA formation, and microbial structure in the AD of FW. In addition, machine learning (ML) has become an effective analytical tool for analyzing AD processes.[14] The ML model constructed by artificial neural network (ANNs) and random forest (RF) is able to predict the methane output without understanding the process mechanism.[15–17] Therefore, we conducted an in-depth exploration of the data through the ML model to determine the key parameters that have a significant impact on AD. Finally, the range values of these parameters were predicted using the model. These studies will provide novel additives with practical application prospects for the AD of FW, and provide reference for parameter optimization methods.

2. Materials and methods

2.1 The additives, FW and inocula

The additives comprised three materials: metal material, porous material, and adhesive. These materials are mixed at a ratio of 5 : 4 : 1 and prepared by a specific method.

The inoculum is taken from an FW treatment plant in Beijing, and the FW is obtained from a school canteen (China University of Petroleum (Beijing), Changing, Beijing). Table 1 shows the physicochemical indicators of the FW and inocula.

2.2 Experimental setup

The semicontinuous AD test was conducted for 138 days. The total volume of the bottle is 1.0 L, and the working volume is 0.8 L.[18] All of the bottles are placed in a shaker (60 rpm) and maintained at 37.0 °C.[19] Feed and discharge were conducted every three days. After each feeding and discharge, the bottle was supplemented with deionized water to maintain the working volume at 0.8 L, and then pumped with N_2 for 8 min. The four reactors were named "no additives", "A1", "A2", and "A3". No additives were added to the "No additives" group. The additive added in group A1 was 1% of the mass of FW (0.08 g, 0.16 g, 0.24 g, 0.32 g, and 0.40 g were added in each of the 5 stages during the experiment). Group A2 added 1.2 g (0.5 g L^{-1}) of the additives each time, while group A3 added 2.4 g (1.0 g L^{-1}) of the additives each time.[20]

Table 1 Physicochemical indicators of FW and inocula

Test materials	pH	TS (%)	VS (%)	VS/TS
FW	5.62	29.59 ± 1.23	28.16 ± 0.85	0.95
Inoculum	7.64	3.69 ± 0.24	1.73 ± 0.17	0.47

2.3 Analyses methods

A gas chromatograph (GC, FULI 9790 II, China) and wet gas flowmeter (LMF-1, China) were used to detect the composition and content of biogas. The GC was equipped with a thermal conductivity detector (TCD), which was connected to a TDX-01 packed column (3 mm × 3 m in inner diameter × length) for detecting CH_4. When the column temperature reached 130 °C, 1.0 mL of the test gas was injected into the detector inlet for analysis.[21] The total solids (TS) and volatile solids (VS) were determined according to Nie's method.[22]

The VFA content was determined using gas chromatography (Agilent 7890B, USA). The sample was first centrifuged for 8–10 min by a high-speed centrifuge (10 000 rpm, 10 °C), and then 1.0 mL of the supernatant was taken and diluted by 5–10 times with ethanol. The diluted sample was filtered with 0.5 μm filter, and analyzed using GC.[23]

2.4 Machine learning methods

Seven experimental variables related to the methane yield (OLR, the additive concentration, VFA, acetic acid, pH, ammonia nitrogen) were selected as the input variables in this study.[24] The total sample size of the data was 160 entries. First, the Pearson correlation coefficient matrix (PCC) preliminarily explored the relationship between the data variables. Second, two ML algorithms (RF and ANN) widely used in AD were designed to model and analyze the experimental data. Python's sklearn library implemented the RF algorithm, and Python implemented the ANN algorithm in the form of a multilayer perceptron (MLP). The two algorithms determined the optimal parameters of the model through Randomsearchcv in the Python sklearn library.[25]

The sklearn module in Python (3.8) was used to speed up the model's training. The data were normalized to a similar scale and normal distribution using the StandardScaler normalization method according to eqn (1). The normalized dataset was randomly classified as a training set (80%) and a test set (20%). The coefficient of determination (R^2) and the root mean square error (RMSE) represent an objective assessment of the predictive accuracy of the ML model performance. Eqn (2) and (3) were used to calculate R^2 and RMSE, respectively.

In addition, feature importance analysis and Shapley additive explanation (SHAP) value analysis were carried out on the optimal model to determine the most critical factors affecting

the methane yield. Finally, the range of optimal variables was determined by a partial dependence plot (PDP) to better optimize the process conditions.

$$x^* = \frac{xi - \overline{x}}{\sigma(x)} \quad (1)$$

$$R^2 = \frac{\sum_{i=1}^{n} (oi - pi)^2 (pi - \overline{p})^2}{\sum_{i=1}^{n} (oi - pi)^2 \sum_{i=1}^{n} (pi - \overline{p})^2} \quad (2)$$

$$\mathrm{RMSE} = \sqrt{\frac{1}{n} \sum_{i=1}^{n} (oi - pi)^2} \quad (3)$$

2.5 Statistical analysis

Single-factor analysis of variance (ANOVA) in IBM SPSS Statistics 26 was used for statistical analysis of the results of this study. Origin 2022b was used to convert the data into figures.

3. Results and discussion

3.1 Characterization of the additives

To investigate the effect of the material structure on the anaerobic microorganisms, the morphology and structure of the additives were analyzed using a scanning electron microscope (SEM). Fig. S1† shows that the additives exhibit an irregular block-like structure with many edges and pore structures on the surface. Many flocculent agglomerated particles are attached to the surface, which may be due to the metal material adhering to the porous material. These particle structures have increased the surface area of the original material. The agglomerated particles and pore structures provide a suitable environment for the attachment and growth of microorganisms.[26]

The nitrogen adsorption–desorption isotherm curves of the metal material and the additives are shown in Fig. S2.† The nitrogen adsorption–desorption isotherms of the metal material and the additives are type IV, indicating that the additives appear as vacancy condensation, and it can be inferred that they possess many mesopores.[27] Table S1† provides the pore structure parameters of different samples. Compared with the metal material, the additives' specific surface area, pore capacity, and average pore size have increased. The specific surface area of the additives was 5.34 times greater than that of the metal material. This phenomenon is mainly due to mixing the metal material with the porous material and adhesive. In addition, the porous material, as a ESI,† increases the specific surface area, pore capacity, and pore size of the original material. In brief, the larger specific surface area can attach more methanogens, which is conducive for enhancing the DIET process of AD.[28]

Furthermore, XPS was used to analyze the elemental valence and chemical groups on the surfaces of the metal materials and the additives.[29] The results showed that Fe, Al, Si, and O are the main elements for composition. Fig. S3(a)† shows that the full scan spectrum of the metal material exhibits the characteristic peaks of Fe 2p and O 1s, indicating the formation of iron oxides on the surface. Fig. S3(b)† shows the Fe 2p spectrum of the metal material. There are two peaks at the binding energy of 710.7 eV and 724.2 eV, representing Fe $2p_{3/2}$ and Fe $2p_{1/2}$, respectively.[30] This indicates that the surface of the metal material is mainly composed of Fe_2O_3.

The full scan spectrum (Fig. S3(c)†) of the additives shows the characteristic peaks of Fe 2p, Al 2p, Si 2p, and O 1s, indicating the formation of iron oxide, aluminum oxide, and silicon oxide on the surface.

Fig. S3(d)† is the Fe 2p spectrum of the additives. There are two peaks at the binding energy of 710.6 eV (Fe $2p_{3/2}$) and 723.8 eV (Fe $2p_{1/2}$), indicating that FeO exists on the surface of the additives. The peaks present at 712.7 eV and 725.9 eV were confirmed as Fe $2p_{3/2}$ and Fe $2p_{1/2}$, respectively, indicating the presence of Fe_2O_3 on the surface of the additives. These results indicate that the additive surface mainly exists in the form of FeO and Fe_2O_3. In addition, the crystal structure and phase composition of the additives were detected *via* XRD (Fig. S4†). XRD diffraction shows that the representative peak of the additives is Fe, and no iron oxide has been detected.[31] The above analysis indicated that the metal material reacted with oxygen in the air or with porous material and adhesive during the synthesis process of the additives, resulting in the formation of iron oxides on the surface. However, not all reactions occur internally, thus retaining the elemental iron. Ultimately, there are iron oxides on the surface of the additives, while the main component inside is elemental iron.

3.2 The effect of the additives on the biogas yield

When the OLR is 1.0, 2.0, 3.0, 4.0, and 5.0 g VS per L per day, the biogas and methane yield of AD in each group is shown in Fig. 1(a) and (c), and the average biogas and methane yield at the stable stage is shown in Fig. 1(b)–(d) and Table 2. When the OLR was 1.0–2.0 g VS per L per day, the biogas and methane yield of each group decreased, indicating that the activity of the microorganism varied with changes in the OLR. However, as the OLR increases to 2.0–3.0 g VS per L per day, the biogas and methane yield increases, which means that the microorganisms adapt to higher OLR.[32] Subsequently, when the OLR continued to increase to 4.0 g VS per L per day, the biogas and methane yield of A2 and A3 decreased, but remained higher than "No additives" and "A1". At this time, the additives still had a promoting effect. The promoting effect may be attributed to the porous structure and surface functional groups within, which facilitated DIET. Related research found that Fe_2O_3 plays a positive role in promoting this process.[33] When the OLR increased from 4.0 to 5.0 g VS per L per day, and the biogas and methane yield of all groups rapidly decreased. With the increased OLR, the methanogens were inhibited, which may be attributed to the excessive accumulation of VFA.[34] Statistical analysis showed (Fig. 2) that there was significant difference in the methane yield between A2 and A3 ($p < 0.05$) when the OLR was 3.0 g VS per L per day and 4.0 g VS per L per day (Fig. 2(c) and (d)). When the OLR was 3.0 g VS per L per day, the methane

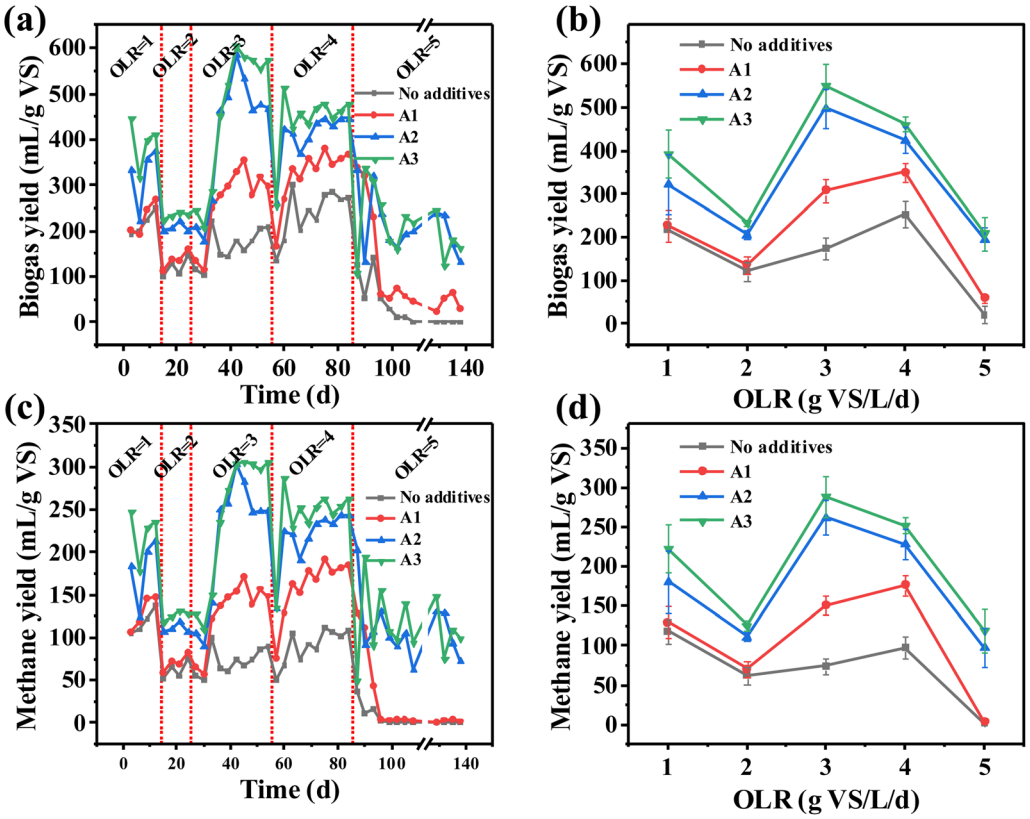

Fig. 1 (a) Daily biogas and (c) methane yields; (b) average biogas and (d) methane yield of AD in steady-state under different OLR.

Table 2 Average biogas and methane yield of AD in steady-state under different OLR

	OLR (g VS per L per day)	1	2	3	4	5
Biogas yield (mL per g VS)	No additives	217 ± 26	121 ± 21	175 ± 26	253 ± 31	21 ± 21
	A1	227 ± 36	136 ± 20	308 ± 28	351 ± 22	59 ± 11
	A2	323 ± 68	207 ± 9	498 ± 46	425 ± 30	196 ± 28
	A3	394 ± 55	234 ± 8	551 ± 51	462 ± 17	209 ± 39
Methane yield (mL per g VS)	No additives	118 ± 15	62 ± 11	74 ± 11	97 ± 14	1 ± 1
	A1	129 ± 20	71 ± 10	151 ± 12	176 ± 13	4 ± 1
	A2	181 ± 39	111 ± 6	263 ± 22	229 ± 19	98 ± 25
	A3	223 ± 31	126 ± 6	289 ± 26	252 ± 11	119 ± 28

yield of A2 and A3 is higher than 4.0 g VS per L per day (Fig. 1(d)). At 3.0 g VS per L per day, there was a significant difference between the methane yield of each group ($p < 0.05$) (Fig. 2(g)). A3 has the highest methane yield at 289 ± 26 mL per g VS (Table 2), which is 9.9% higher than that for A2. However, the additive concentration of A2 was only 50% of that of A3. We considered that 3.0 g VS per L per day OLR and 0.5 g VS per L per day additives were the optimal conditions for economy and maintaining high methane yield.

3.3 The effect of the additives on VFA, conductivity, and ammonia nitrogen

We evaluated the effect of the additives on the AD performance under different OLR and additive concentrations (Fig. 3 and Table 3). When the OLR increased from 1.0 VS per L per day to 4.0 g VS per L per day, VFA remained below 3000 mg L^{-1}. At this point, AD can continue to run under this load.[35] When the OLR increased from 4.0 g VS per L per day to 5.0 g VS per L per day, the VFA of each group exceeded 3000 mg L^{-1}, and the methane yield declined (Fig. 1(d)). It showed that the methanogen was inhibited. At 3.0 g VS per L per day OLR, the VFA and acetic acid contents of A2 and A3 were higher than the groups without the additives. The higher VFA content indicates that the additive promotes hydrolysis and acidification. From 1.0 g VS per L per day to 4.0 g VS per L per day, the pH improved from 7.5 to 7.7 in A2 and A3, and it remained at 7.5 without additives (Fig. 3(e) and Table 3).

Digestate with higher pH values can be used as natural buffers.[36] Therefore, there was no inhibition at OLR 1.0–4.0 g VS per L per day. With the OLR increased from 4.0 g VS per L per

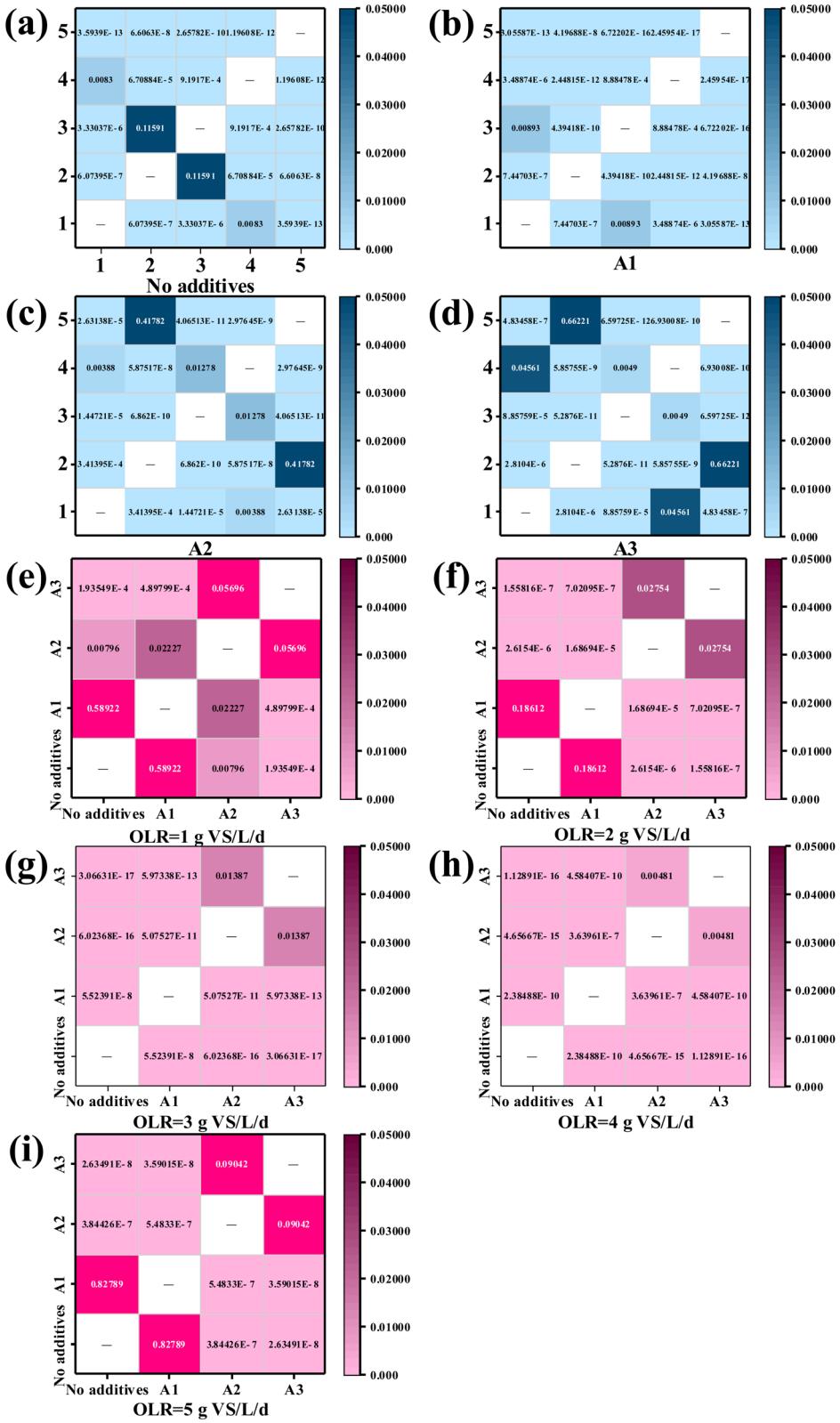

Fig. 2 Significant differences between the different OLR (a–d) and the additive concentrations (e–i).

day to 5.0 g VS per L per day, the pH value of each group sharply decreased to below 6.0. The decrease in pH indicated the accumulation of VFA (Fig. 3(a)–(c)), which inhibited the methanogenesis and led to the decrease in methane yield (Fig. 1(d)).[37] At OLR 4.0 g VS per L per day, the conductivity of the A1, A2, and A3 groups was higher than that of the group without

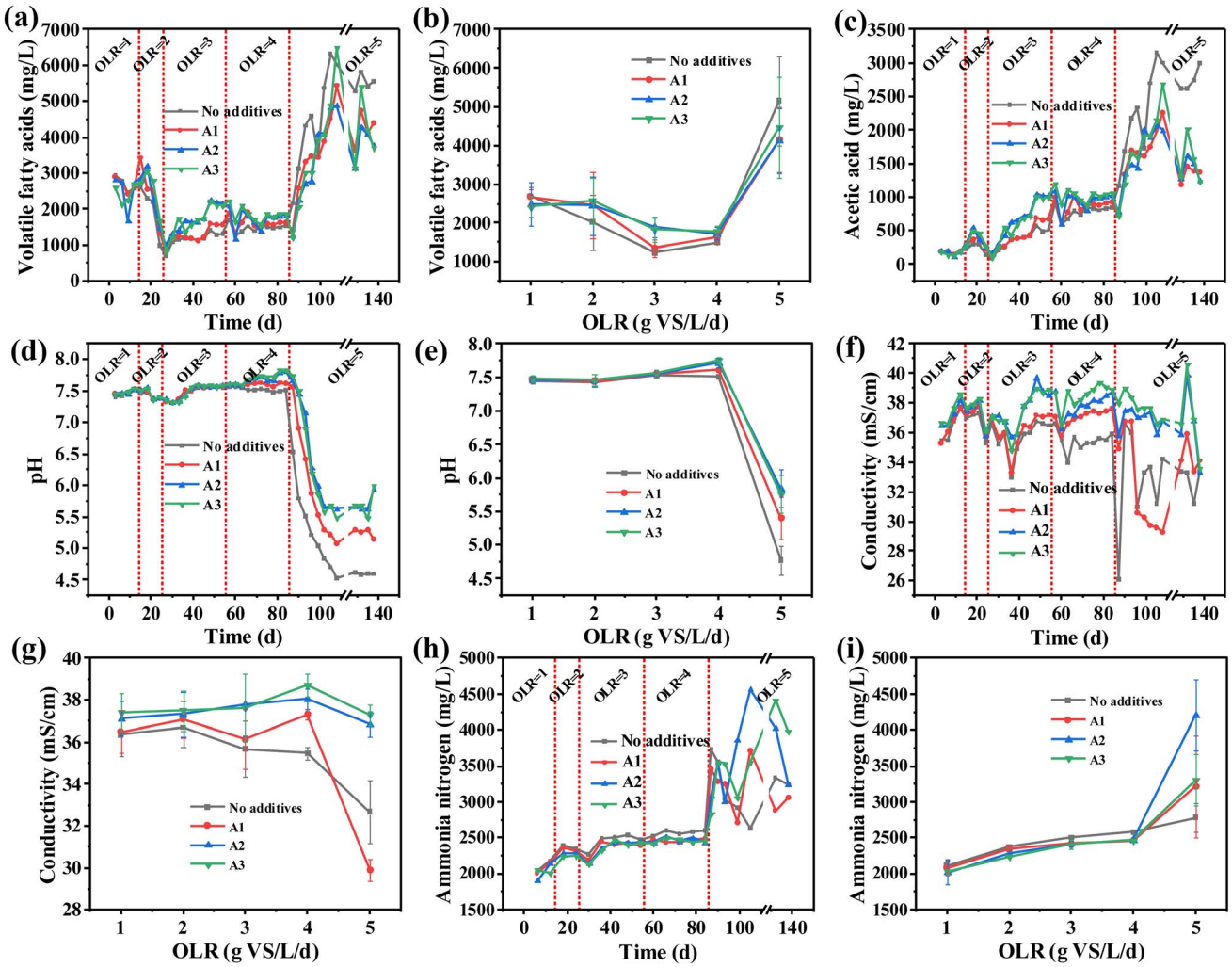

Fig. 3 Variation of VFA, acetic acid, pH, conductivity and ammonia nitrogen. (a) Daily VFA, (c) acetic acid, (d) pH, (f) conductivity, and (h) ammonia nitrogen; (b) average VFA, (e) pH, (g) conductivity, and (i) ammonia nitrogen of AD in steady-state under different OLR.

the additives. The A3 group was provided with the highest conductivity and methane yield. These results indicated that the conductivity and methane yield increased with increasing additive concentration. The reason for the increased electrical conductivity was that the addition of iron elements resulted in the composite material having a certain degree of conductivity. As mentioned earlier, the XPS results showed the presence of elemental iron in the interior of the additive, and iron oxide on the surface. The increase in methane yield may be attributed to more electrons being used for methanogenesis through DIET.[38] The OLR varied from 1.0 g VS per L per day to 4.0 g VS per L per day, and the concentration of ammonia nitrogen in all groups was maintained below 2500 mg L^{-1} (Fig. 3(h), (i) and Table 3). Upon increasing from 4.0 g VS per L per day to 5.0 g VS per L per day, the concentrations of ammonia nitrogen in A1, A2, and A3 increased rapidly, exceeding 3000 mg L^{-1}. At this time, the methane yields significantly decreased. Previous studies have shown that the high ammonia nitrogen concentration inhibited the performance of the methanogens.[39] In summary, the potential promoting effect of the additives increases the OLR to 4.0 g VS per L per day in AD.

3.4 Microbial community analysis

Fig. 4(a) shows the composition of the methanogen in each group under different OLR. The main archaea in each group were *Metanosarcinales* and *Metanomicrobiales*, among which *Metanosarcinales* was the dominant archaea. When the OLR was below 2.0 g VS per L per day, the composition of archaea in each group was consistent, and the abundance of *Methanosarcinales* in the group with the additives was slightly higher than that without. At OLR 3.0 g VS per L per day, the abundance of *Methanosarcinales* in the "no additives", A1, A2, and A3 groups was 91.31%, 91.49%, 92.26%, and 93.35%, respectively. The abundance of *Methanosarcinales* in each group increased with increasing additive concentration. At 4.0 g VS per L per day, the abundance of *Methanosarcinales* in the "no additives", A1, A2, and A3 groups was 62.24%, 64.83%, 80.83%, and 88.07%, respectively. At 5.0 g VS per L per day, the abundance of

Table 3 Average VFA, acetic acid, pH, conductivity, and ammonia nitrogen of AD in steady-state under different OLR

	OLR (g VS per L per day)	1	2	3	4	5
VFA (mg L^{-1})	No additives	2692 ± 225	2023 ± 713	1240 ± 99	1493 ± 54	5155 ± 1148
	A1	2666 ± 202	2462 ± 853	1349 ± 215	1624 ± 132	4150 ± 847
	A2	2495 ± 556	2450 ± 761	1898 ± 277	1720 ± 162	4137 ± 849
	A3	2420 ± 270	2574 ± 603	1830 ± 315	1792 ± 127	4481 ± 1300
Acetic acid (mg L^{-1})	No additives	184 ± 21	243 ± 74	449 ± 77	812 ± 35	2585 ± 569
	A1	185 ± 24	324 ± 78	515 ± 151	900 ± 68	1853 ± 272
	A2	175 ± 37	373 ± 123	831 ± 189	962 ± 75	1882 ± 258
	A3	166 ± 24	385 ± 115	773 ± 227	1011 ± 67	2051 ± 410
pH	No additives	7.45 ± 0.04	7.43 ± 0.05	7.53 ± 0.04	7.51 ± 0.02	4.78 ± 0.22
	A1	7.48 ± 0.04	7.43 ± 0.07	7.55 ± 0.03	7.61 ± 0.02	5.40 ± 0.32
	A2	7.47 ± 0.04	7.46 ± 0.09	7.55 ± 0.06	7.72 ± 0.06	5.84 ± 0.29
	A3	7.49 ± 0.04	7.46 ± 0.09	7.56 ± 0.06	7.75 ± 0.05	5.76 ± 0.28
Conductivity (mS cm^{-1})	No additives	36.35 ± 1.03	36.70 ± 0.94	35.67 ± 1.34	35.47 ± 0.30	32.68 ± 1.48
	A1	36.50 ± 1.03	37.08 ± 0.88	36.14 ± 1.42	37.31 ± 0.25	29.90 ± 0.53
	A2	37.13 ± 0.81	37.33 ± 1.06	37.80 ± 1.49	38.06 ± 0.49	36.86 ± 0.58
	A3	37.40 ± 0.94	37.50 ± 0.97	37.64 ± 1.62	38.71 ± 0.52	37.30 ± 0.51
Ammonia nitrogen (mg L^{-1})	No additives	2115 ± 92	2378 ± 32	2505 ± 30	2585 ± 24	2780 ± 198
	A1	2080 ± 99	2340 ± 28	2423 ± 22	2464 ± 24	3220 ± 707
	A2	2020 ± 170	2281 ± 1	2418 ± 46	2476 ± 38	4210 ± 495
	A3	2030 ± 28	2243 ± 4	2405 ± 64	2468 ± 27	3310 ± 354

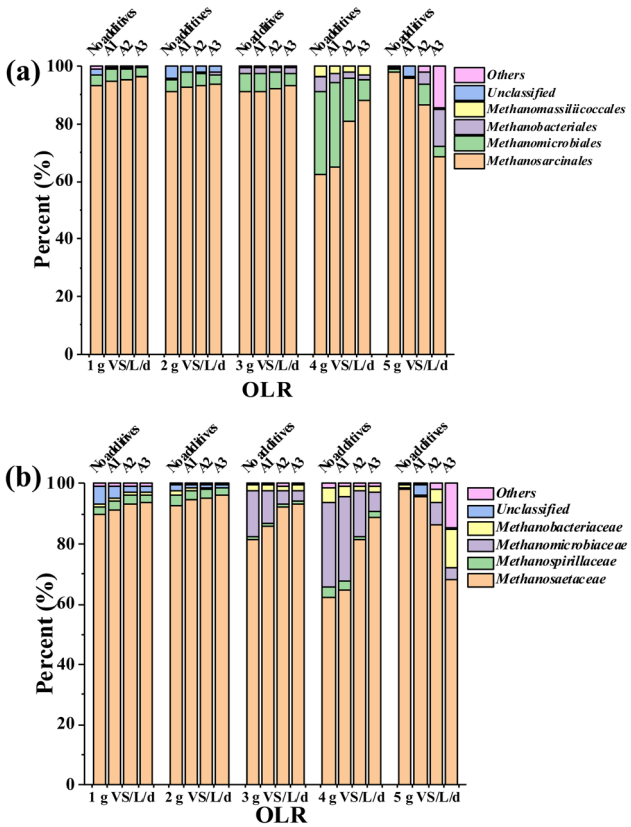

Fig. 4 Compositions of methanogen at the (a) order and (b) family levels under different OLR and the additive concentrations.

Methanosarcinales in the "no additives", A1, A2, and A3 groups was 98.09%, 95.84%, 86.55%, and 68.39%, respectively. When the OLR increased from 1.0 g VS per L per day to 4.0 g VS per L per day, the abundance of *Methanosarcinales* in each group decreased to a certain extent with the increase of OLR, although the trend of decline was most evident in the group without the additives. In 2014, *Metanosarcina* was confirmed to be able to accept electrons and reduce CO_2 to CH_4 through DIET.[9] Furthermore, it can use acetic acid or H_2/CO_2 to produce CH_4. In high-load AD systems, it is usually the dominant archaea community.[40] Due to the increased abundance of *Methanosarcinales*, the additives have the potential to significantly promote DIET in the AD system. Furthermore, additives with mesoporous structures (Fig. S2†) can provide a suitable habitat for microorganisms, which was one of the significant reasons for enhancing the abundance of the dominant species.[28]

Fig. 4(b) shows the composition of methanogens in each group at the family level under different OLR. The main archaea were *Methanosaetaceae* and Methanomicrobiaceae, with *Methanosaetaceae* being the dominant archaea. *Methanosaetaceae* is one of the two known acetoclastic methanogens.[41] The community structure suggested that the acetoclastic methanogenesis pathway was the main pathway in semicontinuous AD. When OLR was 3.0 g VS per L per day, the abundance of *Methanosaetaceae* in the groups "no additives", A1, A2, and A3 was 81.24%, 85.42%, 92.14%, and 93.25%, respectively. The abundance of *Methanosaetaceae* in each group increased with the additive concentration. At 4.0 g VS per L per day, the abundance of *Methanosaetaceae* in the groups "No additives", A1, A2, and A3 was 62.21%, 64.76%, 80.57% and 88.02%, respectively. At 5.0 g VS per L per day, the abundance of *Methanosaetaceae* in the groups "No additives", A1, A2 and A3 was 98.09%, 95.84%, 86.55%, and 68.39%, respectively. The abundance of *Methanosaetaceae* was the highest in the "no additives" group and the lowest in the A3 group. This phenomenon may be due to the rapid increase in VFA when the OLR increases to 5.0 g VS per L per day. At this point, the AD system is already in an unstable state. In summary, at OLR 1.0–4.0 g VS per L per day,

the additives maintained the activity of acetoclastic methanogens with the increased OLR, thereby promoting the conversion of acetic acid to methane. The higher the concentration of the additives, the more pronounced the effect.

3.5 ML analysis

The correlation between the data was preliminarily explored through PCC. The results showed that the pH value and additive concentration were positively correlated with the methane yield. In contrast, the OLR, VFA, acetic acid, and ammonia nitrogen were negatively correlated with the methane yield (Fig. 5(a)). The PCC can find the linear correlation between the data. However, it cannot perform a nonlinear analysis of variables or deeper data relationship mining. Therefore, two ML algorithms, RF and ANN, which are most widely used in AD, are used to predict and analyze the experimental data.[14]

The best combination of RF and ANN was obtained by RandomSearchCV.[42] The RF hyperparameter combination is n_estimators = 314, max_depth = 12, and the ANN hyperparameter combination is hidden_layer_sizes = (100 100), solver = "lbfgs", and activation = 'relu'.

For the prediction of the methane yield, the results show that although the fitting degree of RF in the training set is slightly lower than that of ANN, the fitting degree of RF in the test set is much higher than that of ANN, which may be due to the partial overfitting of ANN. Therefore, compared with the ANN model, RF has superior prediction and generalization performance (higher R^2 and lower RMSE) (Fig. 5(b) and (c)). A comparison of the predicted and actual values for each target, based on the RF model, is shown in Fig. 5(a) and (b). The predicted and actual values are almost always concentrated on the parity line (function $y = x$), with closer points to the parity line indicating higher prediction accuracy. The confidence of the training and test data is set at 95%. The probability that the value is in the purple or blue area is high. The smaller the confidence interval area, the lower the data value uncertainty. In addition, the training set has a higher accuracy and density of distribution around the dichotomous line than the test set. This indicates that the predictions of the training set tend to outperform those of the test set due to the inherent characteristics of the ML algorithm.

Based on the best RF model, the importance of the input characteristics on the methane yield was investigated using the importance analysis method of the self-contained model characteristics and the SHAP method. The importance ranking of the input features generated by the two feature analysis methods showed highly similar results (Fig. 5(d) and (e)). The pH and additive concentration are two key characteristics. The hydrolysis and acidification of organic matter is a crucial limiting step in the AD process, and the composition of VFA in the AD process is mainly affected by pH.[43,44] The additive concentration may mainly affect the abundance of microorganisms, and thus affect the methane yield. As one of the most critical control conditions of the experiment, OLR does not play a significant role in anticipating the methane yield. The relationship between OLR and the methane yield may be explored through partial correlation since OLR is at a fixed state in much of the data, and its range of fluctuation is not as dramatic as other features. Therefore, the relationship between OLR and the methane yield was explored through partial correlation.

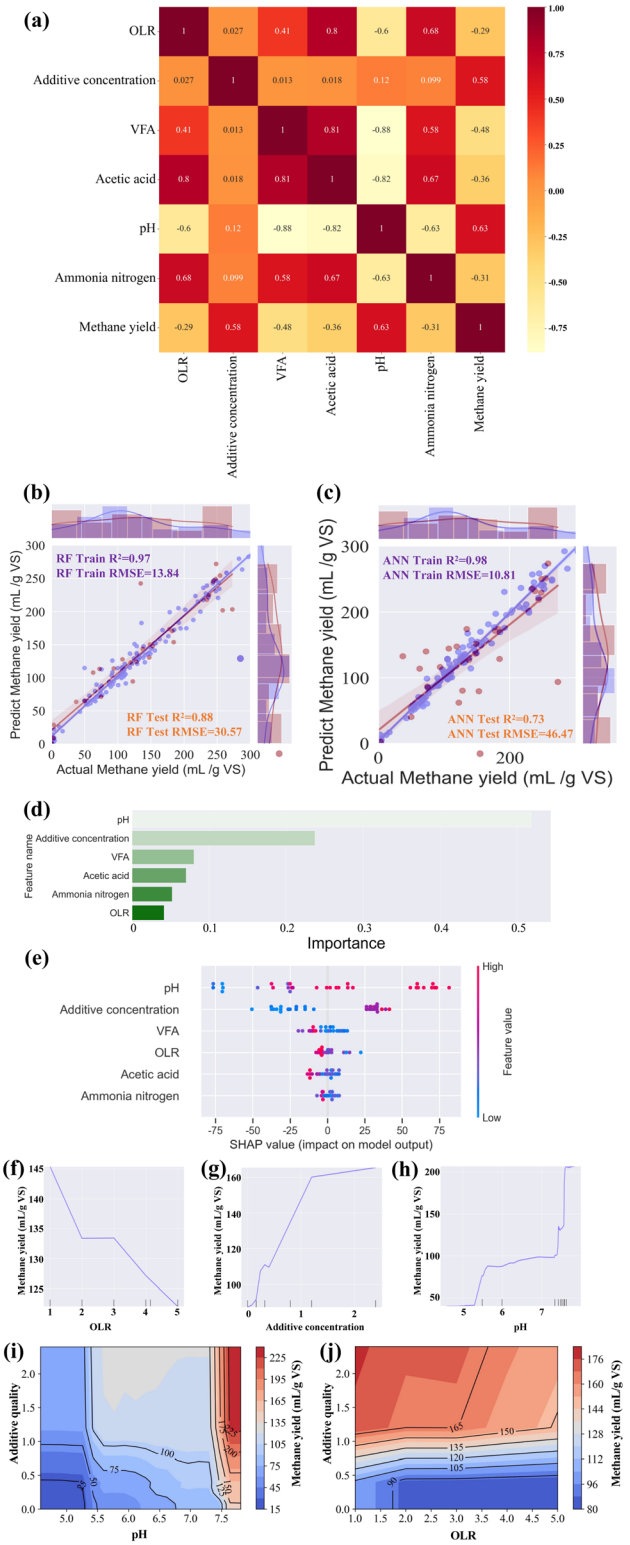

Fig. 5 Plot of Pearson's coefficient of variables (a). ML prediction plot (b and c). Feature importance plot (d and e). 1D partial correlation plot (f–h). 2D partial correlation (i and j).

A one-dimensional partial correlation was carried out using the best RF model to establish the changing relationship between the input variables and methane yield (Fig. 5(f)–(h)). When the pH exceeds 7.6, the maximum promotion effect on the methane yield is achieved. When the pH is 7.5 and below, the promotion effect on the methane yield will sharply drop. This may be because the free VFA can cross the cell membrane of the microorganisms, and dissociate within the cell when the pH is low. The H^+ and ionized VFA acidify the cytoplasm and weaken the cell activity, affecting the efficiency of the methane yield. The inhibition of VFA was attributed to the concentration of free VFA, H^+, and ionized VFA in the system.[45] When the additive concentration is 0–1.5 g, the methane yield rises sharply with increasing additive concentration. It is possible that as the abundance of the microorganisms is affected by the increase in the additive concentration, the increased activity of the acetic acid-consuming methanogenic bacteria promotes the conversion of acetic acid to methane, which in turn increases the methane yield. However, when it is more than 1.5 g, the additive concentration has little impact on the methane yield and gradually enters a stable stage. When the OLR increases, the methane yield gradually decreases. This is probably due to the fast VFA production rate and high nitrogen content of FW, which makes it susceptible to the suppression of VFA or ammonia nitrogen in AD. Therefore, to avoid the inhibition of metabolites such as VFA or ammonia nitrogen, the usual AD reactor can only be operated at a low OLR.

Two-dimensional partial correlation analysis was carried out on the optimal RF model to determine the optimal variable range and its combination. When the pH is between 7.6 and 8.0 and the additive concentration is more than 1.2 g, the maximum promotion effect on the methane yield can be achieved (Fig. 5(i)). When the OLR is between 0 and 3.0 g VS per L per day and the additive concentration is more than 1.1 g, the methane yield can be improved. The ML analysis showed that the experiment achieves optimal daily methane yield in the OLR range of 0–3.0 g VS per L per day, a pH range of 7.6–8.0, and an additive quality of more than 1.2 g (0.5 g per L per day).

4. Conclusion

In this study, we synthesized the additives for promoting the AD of FW. When the OLR was 3.0 g VS per L per day and the additive concentration was 0.5 g VS per L per day, the AD system was able to operate stably, with a methane yield of 263 $\pm$ 22 mL per g VS. In addition, the additives regulated the ammonia nitrogen concentration in high OLR systems to not exceed 2500 mg L^{-1}. This concentration alleviated the inhibition of methanogenesis. The microbial analysis showed that acetoclastic methanogens, *Methanosaetaceae*, was the dominant archaea. Through ML analysis, when the OLR was within the range of 0–3.0 g VS per L per day, the pH was within the range of 7.6–8.0, and the additive concentration was more than 0.5 g per L per day, the optimal daily methane yield would be achieved.

Conflicts of interest

The authors do not have permission to share data.

Acknowledgements

The study was funded by the National Natural Science Foundation of China (General Program, No. 22278435), the Strategic Cooperation Technology Projects of CNPC and CUPB (Grant No. ZLZX2020-04), and the Project of the Joint Research Institute of Carbon Neutrality, State Key Laboratory of Heavy Oil Processing (CUPB-SH-2-02, CNIF20230102).

Notes and references

1 Q. Meng, H. Liu, H. Zhang, S. Xu, E. Lichtfouse and Y. Yun, *Environ. Chem. Lett.*, 2022, **20**, 1745–1762.
2 C. M. Ajay, S. Mohan and P. Dinesha, *Waste Manage.*, 2021, **125**, 10–26.
3 J. O'Connor, S. A. Hoang, L. Bradney, S. Dutta, X. Xiong, D. C. W. Tsang, K. Ramadass, A. Vinu, M. B. Kirkham and N. S. Bolan, *Environ. Pollut.*, 2021, **272**, 115985.
4 H. Wang, J. Xu and L. Sheng, *Energy*, 2019, **173**, 263–277.
5 E. U. Kiran, A. P. Trzcinski, W. J. Ng and Y. Liu, *Fuel*, 2014, **134**, 389–399.
6 N. S. Malvankar, M. Vargas, K. P. Nevin, A. E. Franks, C. Leang, B.-C. Kim, K. Inoue, T. Mester, S. F. Covalla, J. P. Johnson, V. M. Rotello, M. T. Tuominen and D. R. Lovley, *Nat. Nanotechnol.*, 2011, **6**, 573–579.
7 D. R. Lovley, T. Ueki, T. Zhang, N. S. Malvankar, P. M. Shrestha, K. A. Flanagan, M. Aklujkar, J. E. Butler, L. Giloteaux, A.-E. Rotaru, D. E. Holmes, A. E. Franks, R. Orellana, C. Risso and K. P. Nevin, *Adv. Microb. Physiol.*, 2011, **59**, 1–100.
8 A.-E. Rotaru, P. M. Shrestha, F. Liu, M. Shrestha, D. Shrestha, M. Embree, K. Zengler, C. Wardman, K. P. Nevin and D. R. Lovley, *Energy Environ. Sci.*, 2014, **7**, 408–415.
9 A.-E. Rotaru, P. M. Shrestha, F. Liu, B. Markovaite, S. Chen, K. P. Nevin and D. R. Lovley, *Appl. Environ. Microbiol.*, 2014, **80**, 4599–4605.
10 M. S. Romero-Guiza, J. J. Vila, J. Mata-Alvarez, J. M. Chimenos and S. Astals, *Renewable Sustainable Energy Rev.*, 2016, **58**, 1486–1499.
11 C. Cruz Viggi, S. Rossetti, S. Fazi, P. Paiano, M. Majone and F. Aulenta, *Environ. Sci. Technol.*, 2014, **48**, 7536–7543.
12 F. Lü, C. Luo, L. Shao and P. He, *Water Res.*, 2016, **90**, 34–43.
13 L. Zhuang, J. Ma, Z. Yu, Y. Wang and J. Tang, *Microb. Biotechnol.*, 2018, **11**, 710–720.
14 I. Andrade Cruz, W. Chuenchart, F. Long, K. C. Surendra, L. Renata Santos Andrade, M. Bilal, H. Liu, R. Tavares Figueiredo, S. K. Khanal and L. Fernando Romanholo Ferreira, *Bioresour. Technol.*, 2022, **345**, 126433.
15 M.-C. Chiu, C.-Y. Wen, H.-W. Hsu and W.-C. Wang, *Sustainable Energy Technol. Assess.*, 2022, **52**, 102223.
16 J. Gonçalves Neto, L. Vidal Ozorio, T. C. Campos de Abreu, B. Ferreira dos Santos and F. Pradelle, *Fuel*, 2021, **285**, 119081.
17 Y. Zhang, L. Li, Z. Ren, Y. Yu, Y. Li, J. Pan, Y. Lu, L. Feng, W. Zhang and Y. Han, *Bioresour. Technol.*, 2022, **363**, 127899.
18 L. Zhu, B. Wu, Y. Liu, J. Zhang, R. Deng and L. Gu, *Water Res.*, 2022, **221**, 118801.

19 H. Liu, X. Li, Z. Zhang, L. D. Nghiem, L. Gao and Q. Wang, *Water Res.*, 2021, **202**, 117481.
20 M. Chiappero, F. Berruti, O. Mašek and S. Fiore, *Bioresour. Technol.*, 2021, **340**, 125664.
21 W. He, Y. Wei, J. Xiong, Z. Tang, W. Song, J. Liu and Z. Zhao, *Chem. Eng. J.*, 2022, **433**, 133540.
22 H. Nie, H. F. Jacobi, K. Strach, C. Xu, H. Zhou and J. Liebetrau, *Bioresour. Technol.*, 2015, **178**, 238–246.
23 G. Liu, L. Liu, Y. Huo, Z. Dai, L. Zhang and Q. Wang, *J. Cleaner Prod.*, 2022, **379**, 134777.
24 F. Long, L. Wang, W. Cai, K. Lesnik and H. Liu, *Water Res.*, 2021, **199**, 117182.
25 J.-G. Park, H.-B. Jun and T.-Y. Heo, *Appl. Energy*, 2021, **298**, 117250.
26 Z. Ning, B. Xu, W. Zhong, C. Liu, X. Qin, W. Feng and L. Zhu, *Bioresour. Technol.*, 2022, **348**, 126801.
27 H. Shen, R. Zou, Y. Zhou, X. Guo, Y. Guan, D. Na, J. Zhang, X. Fan and Y. Jiao, *Chin. J. Chem. Eng.*, 2022, **42**, 82–90.
28 G. Baek, D. Kim, Y. Choi, J. Cha and C. Lee, *Renewable Sustainable Energy Rev.*, 2023, **183**, 113503.
29 J. Ren, L. Zheng, Y. Su, P. Meng, Q. Zhou, H. Zeng, T. Zhang and H. Yu, *Chem. Eng. J.*, 2022, **445**, 136778.
30 Z. Xu, E. Zheng, Z. Xiao, H. Shao, Y. Liu and J. Wang, *Chem. Eng. J.*, 2023, **459**, 141543.
31 E. Duquesne, S. Betelu, A. Seron, D. Bricault, M. Goldmann, I. Ignatiadis, D. Limagne, A. Vlad, A. Resta, H. Perrot, O. Sel and C. Debiemme-Chouvy, *J. Mater. Chem. A*, 2022, **10**, 24783–24792.
32 Y. Li, R. Zhang, Y. He, C. Zhang, X. Liu, C. Chen and G. Liu, *Bioresour. Technol.*, 2014, **156**, 342–347.
33 R. Zhu, Y. Chen, T. Zhao, Q. Jiang, H. Wang, L. Zheng, D. Shi, J. Zhai, Q. He and L. Gu, *Bioresour. Technol.*, 2020, **313**, 123603.
34 Y. Jiang, C. Dennehy, P. G. Lawlor, Z. Hu, M. McCabe, P. Cormican, X. Zhan and G. E. Gardiner, *Waste Manage.*, 2018, **79**, 302–311.
35 S. Ghanimeh, C. Abou Khalil, C. Bou Mosleh and C. Habchi, *Waste Manage.*, 2018, **71**, 767–774.
36 M. Ye, J. Liu, C. Ma, Y.-Y. Li, L. Zou, G. Qian and Z. P. Xu, *J. Cleaner Prod.*, 2018, **192**, 316–326.
37 B. Eryildiz, Lukitawesa and M. J. Taherzadeh, *Bioresour. Technol.*, 2020, **302**, 122800.
38 Y. Li, Z. Wang, Z. Jiang, L. Feng, J. Pan, M. Zhu, C. Ma, Z. Jing, H. Jiang, H. Zhou, H. Sun and H. Liu, *Bioresour. Technol.*, 2022, **344**, 126353.
39 J. Procházka, P. Dolejš, J. Máca and M. Dohányos, *Appl. Microbiol. Biotechnol.*, 2012, **93**, 439–447.
40 J. De Vrieze, T. Hennebel, N. Boon and W. Verstraete, *Bioresour. Technol.*, 2012, **112**, 1–9.
41 R. Ni, C. Xu, X. Shi, S. Yang, L. Li, X. Peng and L. Song, *J. Cleaner Prod.*, 2022, **372**, 133758.
42 A. Mishra, S. Raut, K. Sehra, R. P. Singh, S. Wadhera, P. Kasturi, G. J. Saxena and M. Saxena, *Int. J. RF Microw. Comput.-Aided Eng.*, 2022, **32**, e23191.
43 C.-f. Liu, X.-z. Yuan, G.-m. Zeng, W.-w. Li and J. Li, *Bioresour. Technol.*, 2008, **99**, 882–888.
44 J. I. Horiuchi, T. Shimizu, K. Tada, T. Kanno and M. Kobayashi, *Bioresour. Technol.*, 2002, **82**, 209–213.
45 Y. Jiang, C. Dennehy, P. G. Lawlor, Z. Hu, Q. Yang, G. McCarthy, S. P. Tan, X. Zhan and G. E. Gardiner, *Waste Manage.*, 2018, **82**, 231–240.